Energies **2014**, *7*, 7620-7639; doi:10.3390/en7117620

OPEN ACCESS

energies

ISSN 1996-1073

www.mdpi.com/journal/energies

Article

Saturated Adaptive Output-Feedback Power-Level Control for Modular High Temperature Gas-Cooled Reactors

Zhe Dong [1,2]

[1] Institute of Nuclear and New Energy Technology, Tsinghua University, Beijing 100084, China; E-Mail: dongzhe@mail.tsinghua.edu.cn; Tel.: +86-10-6279-6425; Fax: +86-10-6278-4832

[2] Key Laboratory of Advanced Reactor Engineering and Safety, Ministry of Education of China, Beijing 100084, China

External Editor: Erich Schneider

Received: 15 September 2014; in revised form: 11 November 2014 / Accepted: 12 November 2014 / Published: 19 November 2014

Abstract: Small modular reactors (SMRs) are those nuclear fission reactors with electrical output powers of less than 300 MW_e. Due to its inherent safety features, the modular high temperature gas-cooled reactor (MHTGR) has been seen as one of the best candidates for building SMR-based nuclear plants with high safety-level and economical competitive power. Power-level control is crucial in providing grid-appropriation for all types of SMRs. Usually, there exists nonlinearity, parameter uncertainty and control input saturation in the SMR-based plant dynamics. Motivated by this, a novel saturated adaptive output-feedback power-level control of the MHTGR is proposed in this paper. This newly-built control law has the virtues of having relatively neat form, of being strong adaptive to parameter uncertainty and of being able to compensate control input saturation, which are given by constructing Lyapunov functions based upon the shifted-ectropies of neutron kinetics and reactor thermal-hydraulics, giving an online tuning algorithm for the controller parameters and proposing a control input saturation compensator respectively. It is proved theoretically that input-to-state stability (ISS) can be guaranteed for the corresponding closed-loop system. In order to verify the theoretical results, this new control strategy is then applied to the large-range power maneuvering control for the MHTGR of the HTR-PM plant. Numerical simulation results show not only the relationship between regulating performance and control input saturation bound but also the feasibility of applying this saturated adaptive control law practically.

Keywords: small modular reactor; modular high-temperature gas-cooled reactor (MHTGR); grid-appropriation; nonlinear adaptive power-level regulation; input saturation compensation

1. Introduction

Nuclear fission energy is a crucial type of clean energy that can play an important role in meeting the world's increasing energy needs. Safety is the most important issue to the development of the nuclear fission energy industry, which leads to the necessity of developing nuclear reactors with inherent safety features. Small modular reactors (SMRs) are those nuclear fission reactors with electrical output powers of less than 300 MW_e. Due to the low power density and large heat capacity, some SMRs have inherent safety features which are the most advanced feature of these SMR-based plants relative to those conventional nuclear plants and protect these SMRs from the hazards of core-melting, radiological release and Loss of Coolant Accidents (LOCAs) [1,2]. SMRs can offer simpler, safer and standardized modular design by factory-building, smaller initial capital investment, and shorter construction period, and have been viewed by International Atomic Energy Agency (IAEA) as a developing trend in nuclear energy. SMRs could be beneficial in providing electric power to remote areas without transmission or distribution infrastructure, in generating local power for a large population center and in being viable for specific applications such as heat sources for industrial complexes. Through adopting a multi-modular scheme, *i.e.*, multiple SMRs providing steam for one turbine/generator set, the inherent safety features can be applicable to large power plants of any desired power rating.

Figure 1. Schematic View of a MHTGR-based NSSM.

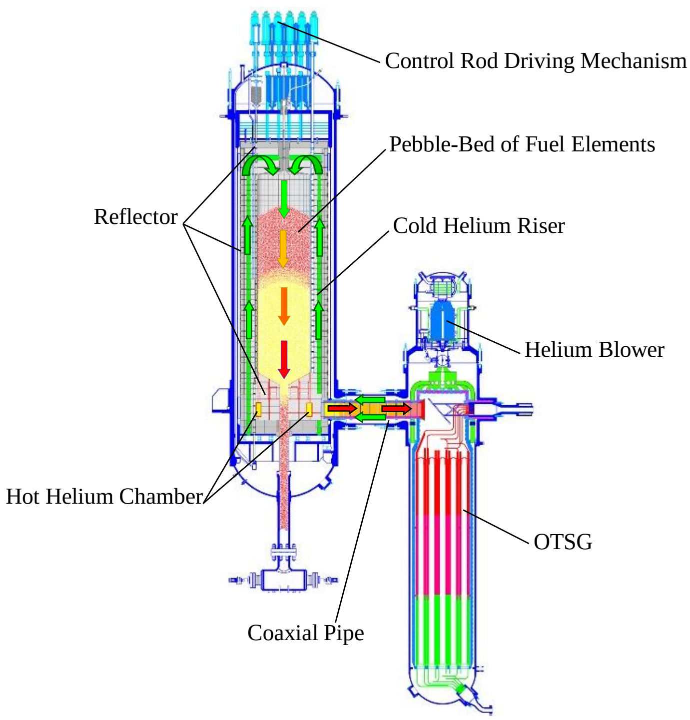

The modular high temperature gas-cooled reactor (MHTGR) such as the HTR-Module designed in Germany [3]), which uses helium as coolant and graphite as both moderator and structural materials, is a typical well known SMR with strong inherent safety features [3,4]. An MHTGR-based nuclear steam supplying module (NSSM) composed of a one-zone pebble-bed MHTGR, a helical-coil once-through steam generator (OTSG) arranged side-by-side with the MHTGR and some connecting pipes, which is the basis of the two-modular nuclear plant HTR-PM developed by the Institute of Nuclear and New Energy Technology and under construction at Tsinghua University [5,6] is shown in Figure 1.

SMRs with load-following capability are grid-appropriate, which can be utilized to incorporate with renewable energy sources such as photovoltaic (PV) and wind to build micro-grids having the virtues of persistent power supply, free refueling of nuclear fission fuels and capability of seawater desalination [7] and hydrogen production [8]. Figure 2 shows a typical micro-grid constituted by an MHTGR-based nuclear plant and a PV plant, from which we can see that the heat produced by the MHTGR can be not only utilized to produce electricity according to the demand signal determined by both the upper-level grid and outlet power of the PV plant but also can be applied for sea-water desalination.

Figure 2. A micro-grid constituted by nuclear fission and photovoltaic energy.

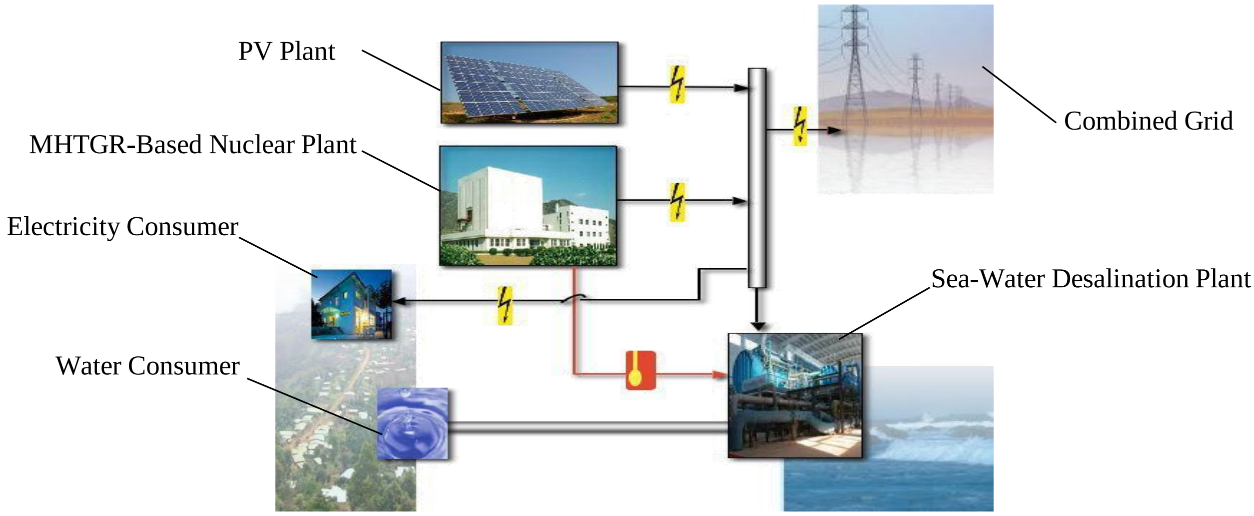

Since the inherent safety features intensify both the dynamic nonlinearity and parameter uncertainty that every fission reactor has, in order to realize the load-following function, it is practically necessary and academically meaningful to develop nonlinear adaptive power-level control for SMRs. Until now, there have been some promising approaches in the nonlinear and adaptive power-level control design. In the nonlinear reactor control field, Shtessel proposed a nonlinear power-level regulator based on sliding mode control and observation techniques for space reactor TOPAZ II [9]. Etchepareborda and Eliasi proposed nonlinear model predictive control (NMPC) design methods for power-level regulation of pressurized water reactors (PWRs) [10–12]. Dong designed a dynamic output feedback dissipation power-level controller for MHTGRs [13] by using a backstepping technique [14]. Based on the physically-based control design approach, Dong proposed a nonlinear dynamic output-feedback power-level control law for MHTGRs [15]. In the field of adaptive reactor control design, Park presented a proportional-integral (PI) power-level controller with feedback gains adjusted by an adaptive law, and this control strategy makes the closed-loop system to be not only stable but also adaptive to the unmodeled reactivity feedback [16]. Arab-Alibeik designed an adaptive power-level controller by using a feedforward artificial neural network (ANN) [17] for the PWRs, and the corresponding ANN is trained online. Dong proposed an ANN-compensated output feedback power-level controller for MHTGRs [18], and the corresponding ANN is a just multi-layer perceptron (MLP) that is trained online by an algorithm given by the need of guaranteeing globally closed-loop stability.

Though strong adaptation ability can be realized based on ANNs, however the implementation of ANN-compensated nonlinear adaptive reactor controllers is much more complicated than that of the widely utilized PID-like control laws. Moreover, there exists saturation element in the control input channel of almost all the practical reactor control systems. Therefore, it is very necessary to design a simple adaptive power-level control laws for the MHTGR by considering control input saturation. In this paper, a novel saturated adaptive output-feedback power-level control is presented, which can not only be adaptive to the perturbation of the physical and thermal-hydraulic parameters but also compensate the control input saturation. It is proved theoretically that this saturated adaptive output-feedback controller can guarantee input-to-state stability (ISS) for the closed-loop system. Furthermore, this newly-built control is simple for practical implementation, and numerical simulation show that it can provide satisfactory power-level regulating performance.

2. Dynamic Model and Problem Formulation

In this section, the nonlinear state-space model for power-level control design is firstly given. Then, after introducing the concept of input-to-stable stability (ISS), the theoretic problem to be solved in the next section is raised.

2.1. Nonlinear State-Space Model for Control Design

From Figure 1, the MHTGR and the OTSG in one NSSM are arranged side by side, and are connected with each other by a horizontal coaxial hot/cold gas duct. Cold helium enters the blower that is mounted on the upper part of the OTSG, and is pressurized before flowing into the cold gas duct. The cold helium enters the channels inside the side-reflector from bottom to top for cooling the reflector, and then passes through the pebble-bed from top to bottom where it is heated to a very high temperature. The hot helium leaves the hot chamber inside the bottom reflector, and then flows into the OTSG primary side where it is cooled to be the cold helium by transferring its heat to the secondary water/steam flow.

By adopting point kinetics with one equivalent delayed neutron group, by considering the temperature feedback effect of the reactor core composed of both the pebble-bed and reflector, and based upon the conservation law of thermal energy, the dynamic model for control design can be written as [15,18]:

$$\begin{cases} \dot{n}_{\mathrm{r}} = \dfrac{\rho_{\mathrm{r}} - \beta}{\Lambda} n_{\mathrm{r}} + \dfrac{\beta}{\Lambda} c_{\mathrm{r}} + \dfrac{\alpha_{\mathrm{R}}}{\Lambda} n_{\mathrm{r}} \left(T_{\mathrm{R}} - T_{\mathrm{R,m}} \right), \\ \dot{c}_{\mathrm{r}} = \lambda \left(n_{\mathrm{r}} - c_{\mathrm{r}} \right), \\ \dot{T}_{\mathrm{R}} = -\dfrac{\Omega_{\mathrm{P}}}{\mu_{\mathrm{R}}} \left(T_{\mathrm{R}} - T_{\mathrm{H}} \right) + \dfrac{P_0}{\mu_{\mathrm{R}}} n_{\mathrm{r}}, \\ \dot{T}_{\mathrm{H}} = \dfrac{\Omega_{\mathrm{P}}}{\mu_{\mathrm{H}}} \left(T_{\mathrm{R}} - T_{\mathrm{H}} \right) - \dfrac{\Omega_{\mathrm{S}}}{\mu_{\mathrm{H}}} \left(T_{\mathrm{H}} - T_{\mathrm{S}} \right), \\ \dot{h}_{\mathrm{r}} = v_{\mathrm{r}}, \end{cases} \tag{1}$$

where:

$$\rho_{\mathrm{r}} = G_{\mathrm{r}} h_{\mathrm{r}} \tag{2}$$

n_r is the relative neutron power; c_r is the relative concentration of the delayed neutron precursor; β is the fraction of the delayed neutrons; Λ is the effective prompt neutron life time; ρ_r is the reactivity provided by the control rods; λ is the effective radioactive decay constant of the delayed neutron precursor; T_R and α_R are respectively the temperature and reactivity feedback coefficient of the reactor core constituted by both the fuel elements and the reflector; $T_{R,m}$ is the initial equilibrium value of T_R; P_0 is the rated thermal power; T_H is the average helium temperature of the primary loop, T_S is the average coolant temperature of the OTSG secondary side; Ω_P is the heat transfer coefficient between the helium and the reactor core; Ω_S is the heat transfer coefficient between the two sides of the OTSG; μ_R and μ_H is respectively the total heat capacities of the reactor core and helium flow inside the primary loop; M_S is the mass flowrate times the heat capacity of the secondary water/steam flow; constant G_r is the differential worth of the control rod; h_r is total control rod position; v_r is the designed control rod speed signal. Here, it is worthy to be noted that α_R is guaranteed to be negative by the physical design of the MHTGR.

Define deviations of n_r, c_r, T_R, T_H, T_S, and h_r from their equilibrium values, *i.e.*, n_{r0}, c_{r0}, T_{R0}, T_{H0}, T_{S0} and h_{r0} as:

$$\begin{cases} \delta n_{\mathrm{r}} = n_{\mathrm{r}} - n_{\mathrm{r0}} \\ \delta c_{\mathrm{r}} = c_{\mathrm{r}} - c_{\mathrm{r0}} \\ \delta T_{\mathrm{R}} = T_{\mathrm{R}} - T_{\mathrm{R0}} \\ \delta T_{\mathrm{H}} = T_{\mathrm{H}} - T_{\mathrm{H0}} \\ \delta T_{\mathrm{S}} = T_{\mathrm{S}} - T_{\mathrm{S0}} \\ \delta h_{\mathrm{r}} = h_{\mathrm{r}} - h_{\mathrm{r0}}. \end{cases} \tag{3}$$

Since δT_S can be well eliminated by the secondary steam temperature controller, it is assumed that:

$$\delta T_{\mathrm{S}} \equiv 0. \tag{4}$$

Then, define:

$$\boldsymbol{x} = \begin{bmatrix} x_1 & x_2 & x_3 & x_4 & x_5 \end{bmatrix}^{\mathrm{T}} = \begin{bmatrix} \delta n_{\mathrm{r}} & \delta c_{\mathrm{r}} & \delta T_{\mathrm{R}} & \delta T_{\mathrm{H}} & \delta T_{\mathrm{S}} \end{bmatrix}^{\mathrm{T}} \tag{5}$$

$$\xi = \delta h_{\mathrm{r}} \tag{6}$$

$$u = v_{\mathrm{r}} \tag{7}$$

and:

$$\boldsymbol{y} = \begin{bmatrix} x_1 & x_4 & \xi \end{bmatrix}^{\mathrm{T}} \tag{8}$$

where $\boldsymbol{x}$ is the state-vector of the NSSM; $[\boldsymbol{x}^{\mathrm{T}}\ \xi]^{\mathrm{T}}$ constitutes the state-vector of the whole system; u is the control input, $\boldsymbol{y}$ is the measured system output.

Based on the above assumption and definition, the nonlinear state-space model for control design can be written as:

$$\begin{cases} \dot{\boldsymbol{x}} = \boldsymbol{f}(\boldsymbol{x}) + \boldsymbol{g}(\boldsymbol{x})\xi, \\ \dot{\xi} = u, \\ \boldsymbol{y} = \boldsymbol{h}(\boldsymbol{x}, \xi), \end{cases} \tag{9}$$

where:

$$\boldsymbol{f}(\boldsymbol{x}) = \begin{bmatrix} -\frac{\beta}{\Lambda}(x_1 - x_2) + \frac{\alpha_R}{\Lambda}(n_{r0} + x_1)x_3 \\ \lambda(x_1 - x_2) \\ \frac{P_0}{\mu_R}x_1 - \frac{\Omega_P}{\mu_R}(x_3 - x_4) \\ \frac{\Omega_P}{\mu_H}(x_3 - x_4) - \frac{\Omega_S}{\mu_H}x_4 \end{bmatrix} \tag{10}$$

$$\boldsymbol{g}(\boldsymbol{x}) = \begin{bmatrix} \frac{G_r}{\Lambda}(n_{r0} + x_1) & \boldsymbol{O}_{1\times 3} \end{bmatrix}^T \tag{11}$$

and:

$$\boldsymbol{h}(\boldsymbol{x}, \xi) = \begin{bmatrix} x_1 & x_4 & \xi \end{bmatrix}^T \tag{12}$$

2.2. Theoretic Problem Formulation

Before giving the theoretic problem, the definition of input-to-state stability (ISS) is introduced.

Definition 1 [19]. Consider a nonlinear system

$$\dot{\boldsymbol{z}} = \boldsymbol{F}(\boldsymbol{z}, \boldsymbol{v}) \tag{13}$$

where $\boldsymbol{z} \in \mathrm{R}^n$ and $\boldsymbol{v} \in \mathrm{R}^m$ are the state and disturbance respectively, and $\boldsymbol{F}$ is locally Lipschiz in $\boldsymbol{z}$ and $\boldsymbol{v}$. System (13) is said to be input-to-state stable if and only if there is a smooth positive definite radially unbounded function U and class K_∞ function σ and ω so that:

$$\frac{\partial U}{\partial \boldsymbol{z}}\boldsymbol{F}(\boldsymbol{z}, \boldsymbol{v}) \le -\sigma(\|\boldsymbol{z}\|) + \omega(\|\boldsymbol{v}\|) \tag{14}$$

Here, a function φ is said to be class K_∞ if it is strictly increasing, φ(0) = 0, and φ(r)→∞ when r→∞.

Remark 1. From Equation (14), it is clear that:

$$\frac{\partial U}{\partial \boldsymbol{z}}\boldsymbol{F}(\boldsymbol{z}, \boldsymbol{v}) \le 0$$

if $\|\boldsymbol{z}\| \ge \sigma^{-1}\omega(\|\boldsymbol{v}\|)$, from which we can see that Definition 1 describes the robustness of system (13) relative to disturbance $\boldsymbol{v}$.

The motivation of introduce the definition of ISS is to deal with the negative effect caused by control input saturation. For compensating the control input saturation and parameter uncertainty, the theoretical problem to be solved is summarized as follows.

Problem 1. How to design a saturated adaptive output feedback control:

$$u = u(\boldsymbol{y}) \tag{15}$$

of system (9) so that the corresponding closed-loop system is input-to-state stable, and:

$$u_{\mathrm{min}} \le u \le u_{\mathrm{max}} \tag{16}$$

where u_{min} is a negative constant, and u_{max} is a positive constant.

3. Saturated Adaptive Output-Feedback Power-Level Control Design

The design result of the saturated adaptive output-feedback power-level control law for the MHTGRs is summarized as the following Theorem 1 which is the main result of this paper and solves Problem 1 raised in the end of Section 2.

Theorem 1. Consider nonlinear system (9) with saturated adaptive output feedback control:

$$u = \mathrm{sat}\left(\dot{\xi}_{\mathrm{d}}\right) + u_{\mathrm{cp}} \tag{17}$$

where:

$$\xi_{\mathrm{d}} = -\left[k_{\mathrm{NP}}x_1 + k_{\mathrm{NI}}\int_0^t x_1(s)\mathrm{d}s\right] - \gamma q_{\mathrm{R}}\left[\hat{\theta}_1 x_4 + \hat{\theta}_2\int_0^t x_4(s)\mathrm{d}s\right] \tag{18}$$

$$\begin{aligned} u_{\mathrm{cp}} = &-k_{\mathrm{g}}\mathrm{th}(e_{\mathrm{g}}) - \left[q_{\mathrm{E1}} + \kappa_{\mathrm{g2}}\kappa_{\mathrm{f3}} - \kappa_{\mathrm{g1}}^2\mathrm{ch}^{-2}\left(\int_{t_0}^t e_\xi(s)\mathrm{d}s\right)\right]\mathrm{th}\left(\int_{t_0}^t e_\xi(s)\mathrm{d}s\right) \\ &+\left[q_{\mathrm{E2}}\kappa_{\mathrm{f1}} + \kappa_{\mathrm{g2}}\kappa_{\mathrm{f3}} + \kappa_{\mathrm{g1}}\kappa_{\mathrm{g2}}\mathrm{ch}^{-2}\left(\int_{t_0}^t e_\xi(s)\mathrm{d}s\right)\right]\mathrm{th}(e_{\mathrm{f}}) \end{aligned} \tag{19}$$

$$e_{\mathrm{g}} = e_\xi + \kappa_{\mathrm{g1}}\mathrm{th}\left(\int_{t_0}^t e_\xi(s)\mathrm{d}s\right) + \kappa_{\mathrm{g2}}\mathrm{th}(e_{\mathrm{f}}) \tag{20}$$

$$\dot{e}_{\mathrm{f}} = \mathrm{ch}^2(e_{\mathrm{f}})\left[-\kappa_{\mathrm{f1}}e_{\mathrm{g}} + \kappa_{\mathrm{f2}}\mathrm{th}\left(\int_0^t e_\xi(s)\mathrm{d}s\right) - \kappa_{\mathrm{f3}}\mathrm{th}(e_{\mathrm{f}})\right] \tag{21}$$

$$e_\xi = \xi - \xi_{\mathrm{d}} \tag{22}$$

$$\mathrm{sat}(z) = \begin{cases} u_{\mathrm{max}} - u_{\mathrm{cp}} & z > u_{\mathrm{max}} - u_{\mathrm{cp}}, \\ z & u_{\mathrm{min}} - u_{\mathrm{cp}} \le z \le u_{\mathrm{max}} - u_{\mathrm{cp}}, \quad z \in \mathrm{R} \\ u_{\mathrm{min}} - u_{\mathrm{cp}} & z < u_{\mathrm{min}} - u_{\mathrm{cp}}, \end{cases} \tag{23}$$

$$\mathrm{th}(z) = \frac{e^z - e^{-z}}{e^z + e^{-z}}, \quad z \in \mathrm{R} \tag{24}$$

$$\mathrm{ch}(z) = \frac{e^z + e^{-z}}{2}, \quad z \in \mathrm{R} \tag{25}$$

k_{NP}, k_{NI}, q_{R}, k_ξ, $\kappa_{\mathrm{g}i}$ ($i = 1, 2$), $\kappa_{\mathrm{f}i}$ ($i = 1, 2, 3$); γ are all given positive constants, $0 < \gamma < 1$; and $\hat{\theta}_i$ ($i = 1, 2$) are online adapted parameters with adaptation law given by:

$$\dot{\hat{\theta}}_1 = \pi_1 \gamma q_R x_1 x_4 \tag{26}$$

$$\dot{\hat{\theta}}_2 = \pi_2 \gamma q_R x_1 \int_{t_0}^{t} x_4(s)\,\mathrm{d}s \tag{27}$$

where π_i (i = 1, 2) are given positive constants. Then, the closed-loop system constituted by (9) and (17) is input-to-state stable if:

$$k_{NP} \geq \frac{q_R P_0 (\Omega_P + \Omega_S)}{2(1-\gamma)\eta G_r \Omega_P \Omega_S} + \varepsilon_{NP} \tag{28}$$

$$\kappa_{f2} = \frac{q_{E1}}{q_{E2}} \kappa_{g2} \tag{29}$$

$$u_{min} < u_{cp} < u_{max} \tag{30}$$

$$\kappa_{g2}\kappa_{f1} - \kappa_{g1} - \frac{G_r}{\varepsilon_{NP}} - \gamma_w > 0 \tag{31}$$

$$q_{E1}\kappa_{g1} - \frac{G_r}{\varepsilon_{NP}} \kappa_{g1}^2 > 0 \tag{32}$$

and:

$$q_{E2}\kappa_{f3} - \frac{G_r}{\varepsilon_{NP}} \kappa_{g2}^2 > 0 \tag{33}$$

where η, q_{Ei} (i = 1, 2), ε_{NP} and γ_w are all given positive constants, and $0 < \eta < 1$.

Before giving the proof of this theorem, the following two useful remarks are firstly given, from which we can preliminarily deduce some properties of newly-built MHTGR power-level control (17).

Remark 2. The term u_{cp} in Equation (17) is just designed for compensating the control input saturation. Because of the boundness of hyperbolic tangent function th(·) given by Equation (24), inequality (30) can be easily satisfied by proper choosing positive scalars k_g, q_{Ei} (i = 1, 2), κ_{gi} (i = 1, 2), κ_{fi} (i = 1, 3).

Remark 3. Due to the boundness of function th(·), it is clear that control input given by Equation (17) satisfies inequality (16), which means that this control is naturally saturated.

Now, the proof the above theorem is presented as follows, which summarizes the design procedure of saturated adaptive output-feedback power-level control law (17).

Proof of Theorem 1. Here, Theorem 1 will be proved in two steps. The first step is to design a virtual adaptive output feedback control ξ_d for subsystem

$$\dot{\boldsymbol{x}} = \boldsymbol{f}(\boldsymbol{x}) + \boldsymbol{g}(\boldsymbol{x})\xi_d \tag{34}$$

where ξ_d is the setpoint of state-variable ξ. The second step is to design adaptive output feedback control input u so that the closed-loop system is globally asymptotically stable and inequality (16) is satisfied.

First, the virtual adaptive output feedback control ξ_d is designed for subsystem (34). Since the shifted-ectropy of the neutron kinetics can be written as [16]:

$$\zeta_N(x_1,x_2)=\Lambda\left[\left(1+\frac{x_1}{n_{r0}}\right)-\ln\left(1+\frac{x_1}{n_{r0}}\right)\right]+\frac{\beta}{\lambda}\left[\left(1+\frac{x_2}{n_{r0}}\right)-\ln\left(1+\frac{x_2}{n_{r0}}\right)\right] \tag{35}$$

the Lyapunov function corresponding to the neutron kinetics can be chosen as

$$V_N(x_1,x_2)=\zeta_N(x_1,x_2)+\frac{G_r k_{NI}}{2}\left[\int_{t_0}^{t}x_1(s)\mathrm{d}s\right]^2 \tag{36}$$

where the second term of V_N denotes the variation of the released fission energy. By differentiating (35) along the trajectory given by the neutron kinetics, we can obtain that:

$$\dot{V}_N(x_1,x_2)=-\frac{\beta(x_1-x_2)^2}{(n_{r0}+x_1)(n_{r0}+x_1)}+x_1\left[G_r\xi_d+\alpha_R x_3+\kappa_I\int_{t_0}^{t}x_1(s)\mathrm{d}s\right] \tag{37}$$

Moreover, it is clear that the shifted-ectropy of the thermal-hydraulic loop is [16]:

$$\zeta_T(x_3,x_4)=\frac{1}{2}\left(\mu_R x_3^2+\mu_H x_4^2\right) \tag{38}$$

and then choose the corresponding Lyapunov function as:

$$V_T(x_3,x_4)=(1-\gamma)\zeta_T(x_3,x_4)+\gamma\varsigma_T(x_3,x_4) \tag{39}$$

where $0<\gamma<1$, and:

$$\varsigma_T(x_3,x_4)=\frac{1}{2\mu_R}\left[\mu_R x_3+\mu_H x_4+\Omega_S\int_{t_0}^{t}x_4(s)\mathrm{d}s\right]^2 \tag{40}$$

denotes the energy variation of the MHTGR thermal-hydraulic loop. Differentiate (39):

$$\begin{aligned}\dot{V}_T(x_3,x_4)=&P_0x_1x_3+\gamma P_0x_1\left[\frac{\mu_H}{\mu_R}x_4+\frac{\Omega_S}{\mu_R}\int_{t_0}^{t}x_4(s)\mathrm{d}s\right]-(1-\gamma)(1-\eta)\left[\Omega_P(x_3-x_4)^2+\Omega_S x_4^2\right]\\&-(1-\gamma)\eta\left[(\Omega_P+\Omega_S)\left(x_4-\frac{\Omega_P}{\Omega_P+\Omega_S}x_3\right)^2+\frac{\Omega_P\Omega_S}{\Omega_P+\Omega_S}x_3^2\right]\end{aligned} \tag{41}$$

where $0<\eta<1$.

Based on the above derivation, choose the Lyapunov function for subsystem (34) as

$$V_1(\boldsymbol{x})=V_N(x_1,x_2)+\frac{q_R}{P_0}V_T(x_3,x_4) \tag{42}$$

and differentiate V_1 along the trajectory given by (34),

$$\dot{V}_1(\boldsymbol{x}) = -\frac{\beta(x_1-x_2)^2}{(n_{r0}+x_1)(n_{r0}+x_1)} - (1-\gamma)(1-\eta)\frac{q_R}{P_0}\left[\Omega_P(x_3-x_4)^2+\Omega_S x_4^2\right]$$
$$-(1-\gamma)\eta(\Omega_P+\Omega_S)\frac{q_R}{P_0}\left(x_4-\frac{\Omega_P}{\Omega_P+\Omega_S}x_3\right)^2 - \frac{q_R}{2\Sigma_R}\left\{x_3^2+\left[x_3-\Sigma_R\left(1+\frac{\alpha_R}{q_R}\right)x_1\right]^2\right\}$$
$$+G_r x_1\left\{\begin{array}{l}\xi_d+\frac{1}{2}\frac{q_R\Sigma_R}{G_r}\left(1+\frac{\alpha_R}{q_R}\right)^2 x_1\\ +k_{NI}\int_{t_0}^{t}x_1(s)\mathrm{d}s+\gamma q_R\left[\frac{\mu_H}{G_r\mu_R}x_4+\frac{\Omega_S}{G_r\mu_R}\int_{t_0}^{t}x_4(s)\mathrm{d}s\right]\end{array}\right\} \tag{43}$$

where:

$$\Sigma_R = \frac{(\Omega_P+\Omega_S)P_0}{(1-\gamma)\eta\Omega_P\Omega_S} \tag{44}$$

$$\theta_1 = \frac{\mu_H}{G_r\mu_R} \tag{45}$$

and:

$$\theta_2 = \frac{\Omega_S}{G_r\mu_R} \tag{46}$$

Here, since scalars θ_i (i = 1, 2) are tightly related to MHTGR physical and thermal parameters which cannot be obtained accurately. By defining $\hat{\theta}_i$ as the estimation of θ_i (i = 1, 2), choose virtual control input ξ_d as Equation (18) where k_{NP} satisfies inequality (28). Then, substitute Equations (18) to (43),

$$\dot{V}_1(\boldsymbol{x}) \le -\frac{\beta(x_1-x_2)^2}{(n_{r0}+x_1)(n_{r0}+x_1)} - G_r\varepsilon_{NP}x_1^2 - (1-\gamma)(1-\eta)\frac{q_R}{P_0}\left[\Omega_P(x_3-x_4)^2+\Omega_S x_4^2\right]$$
$$-(1-\gamma)\eta(\Omega_P+\Omega_S)\frac{q_R}{P_0}\left(x_4-\frac{\Omega_P}{\Omega_P+\Omega_S}x_3\right)^2 - \frac{q_R}{2\Sigma_R}\left\{x_3^2+\left[x_3-\Sigma_R\left(1+\frac{\alpha_R}{q_R}\right)x_1\right]^2\right\} \tag{47}$$
$$-\gamma q_R\left[\tilde{\theta}_1 x_1 x_4+\tilde{\theta}_2 x_1\int_{t_0}^{t}x_4(s)\mathrm{d}s\right],$$

where:

$$\tilde{\theta}_i = \hat{\theta}_i - \theta_i, \quad (i=1,2) \tag{48}$$

are estimation error corresponding to θ_i (i = 1, 2).

To guarantee the stability of the closed-loop formed by subsystem (34) and (18), it is necessary to design a proper online adaptation law of $\hat{\theta}_i$ (i = 1, 2). Thus, define the expanded Lyapunov function as

$$V_2(\boldsymbol{x},\tilde{\theta}) = V_1(\boldsymbol{x}) + \frac{1}{2}\tilde{\theta}^{T}\Pi^{-1}\tilde{\theta} \tag{49}$$

where:

$$\tilde{\theta} = \begin{bmatrix} \tilde{\theta}_1 & \tilde{\theta}_2 \end{bmatrix}^{\mathrm{T}} \tag{50}$$

and:

$$\Pi = \begin{bmatrix} \pi_1 & 0 \\ 0 & \pi_2 \end{bmatrix}, \quad \pi_i > 0, \quad (i = 1, 2) \tag{51}$$

By differentiating V_2, since we can obtain that:

$$\begin{aligned} \dot{V}_2\left(\boldsymbol{x}, \tilde{\theta}\right) \le & -\frac{\beta\left(x_1 - x_2\right)^2}{\left(n_{\mathrm{r}0} + x_1\right)\left(n_{\mathrm{r}0} + x_1\right)} - G_{\mathrm{r}}\varepsilon_{\mathrm{NP}}x_1^2 - (1-\gamma)(1-\eta)\frac{q_{\mathrm{R}}}{P_0}\left[\Omega_{\mathrm{P}}\left(x_3 - x_4\right)^2 + \Omega_{\mathrm{S}}x_4^2\right] \\ & -(1-\gamma)\eta\left(\Omega_{\mathrm{P}} + \Omega_{\mathrm{S}}\right)\frac{q_{\mathrm{R}}}{P_0}\left(x_4 - \frac{\Omega_{\mathrm{P}}}{\Omega_{\mathrm{P}} + \Omega_{\mathrm{S}}}x_3\right)^2 - \frac{q_{\mathrm{R}}}{2\Sigma_{\mathrm{R}}}\left\{x_3^2 + \left[x_3 - \Sigma_{\mathrm{R}}\left(1 + \frac{\alpha_{\mathrm{R}}}{q_{\mathrm{R}}}\right)x_1\right]^2\right\} \\ & -\gamma q_{\mathrm{R}}\left[\tilde{\theta}_1 x_1 x_4 + \tilde{\theta}_2 x_1 \int_{t_0}^{t} x_4(s)\,\mathrm{d}s\right] + \tilde{\theta}^{\mathrm{T}}\Pi^{-1}\dot{\hat{\theta}}. \end{aligned} \tag{52}$$

From inequality (52), it is clear that if the adaptation laws corresponding to $\hat{\theta}_i$ (i = 1, 2) are chosen as (26) and (27), then we have:

$$\begin{aligned} \dot{V}_2\left(\boldsymbol{x}, \tilde{\boldsymbol{\theta}}\right) \le & -\frac{\beta\left(x_1 - x_2\right)^2}{\left(n_{\mathrm{r}0} + x_1\right)\left(n_{\mathrm{r}0} + x_1\right)} - G_{\mathrm{r}}\varepsilon_{\mathrm{NP}}x_1^2 - (1-\gamma)(1-\eta)\frac{q_{\mathrm{R}}}{P_0}\left[\Omega_{\mathrm{P}}\left(x_3 - x_4\right)^2 + \Omega_{\mathrm{S}}x_4^2\right] \\ & -(1-\gamma)\eta\left(\Omega_{\mathrm{P}} + \Omega_{\mathrm{S}}\right)\frac{q_{\mathrm{R}}}{P_0}\left(x_4 - \frac{\Omega_{\mathrm{P}}}{\Omega_{\mathrm{P}} + \Omega_{\mathrm{S}}}x_3\right)^2 - \frac{q_{\mathrm{R}}}{2\Sigma_{\mathrm{R}}}\left\{x_3^2 + \left[x_3 - \Sigma_{\mathrm{R}}\left(1 + \frac{\alpha_{\mathrm{R}}}{q_{\mathrm{R}}}\right)x_1\right]^2\right\} \end{aligned} \tag{53}$$

which means that $\boldsymbol{x} \to \boldsymbol{O}$ as $t \to \infty$. The adaptive virtual control of subsystem (18) can be summarized as

$$\begin{cases} \xi_{\mathrm{d}} = -\left[k_{\mathrm{NP}}x_1 + k_{\mathrm{NI}}\int_{t_0}^{t} x_1(s)\,\mathrm{d}s\right] - \gamma q_{\mathrm{R}}\left[\hat{\theta}_1 x_4 + \hat{\theta}_2 \int_{t_0}^{t} x_4(s)\,\mathrm{d}s\right] \\ \dot{\hat{\theta}}_1 = \pi_1 \gamma q_{\mathrm{R}} x_1 x_4 \\ \dot{\hat{\theta}}_2 = \pi_2 \gamma q_{\mathrm{R}} x_1 \int_{t_0}^{t} x_4(s)\,\mathrm{d}s \end{cases} \tag{54}$$

<u>*Second*,</u> based on virtual control (54), saturated control input u of entire system (9) is designed.

For compensating control input saturation, an expanded state-variable e_{f} is introduced, which satisfies differential Equation (21) and where scalar e_{g} is given by Equation (20). Moreover, set:

$$V_{\mathrm{ex}}\left(e_{\mathrm{f}}, e_g\right) = \frac{1}{2}e_{\mathrm{g}}^2 + q_{\mathrm{E}1}\ln\left[\mathrm{ch}\left(\int_{t_0}^{t} e_{\xi}(s)\,\mathrm{d}s\right)\right] + \frac{1}{2}q_{\mathrm{E}2}\,\mathrm{th}^2\left(e_{\mathrm{f}}\right) \tag{55}$$

which is positive-definite and where $q_{\mathrm{E}i}$ (i = 1,2) are given positive constants. Differentiate V_{ex} along the trajectory given by (21) and (20) and based on Equation (29):

$$\begin{aligned}\dot{V}_{\text{ex}}\left(e_{\text{f}},e_{g}\right)&=e_{\text{g}}\dot{e}_{\text{g}}+q_{\text{E1}}\text{th}\left(\int_{t_0}^{t}e_{\xi}\left(s\right)\text{d}s\right)e_{\xi}+q_{\text{E2}}\,\text{th}\left(e_{\text{f}}\right)\text{ch}^{-2}\left(e_{\text{f}}\right)\dot{e}_{\text{f}}\\&=e_{\text{g}}\left(u-\dot{\xi}_{\text{d}}\right)-\left[\kappa_{\text{g2}}\kappa_{\text{f1}}-\kappa_{\text{g1}}\text{ch}^{-2}\left(\int_{t_0}^{t}e_{\xi}\left(s\right)\text{d}s\right)\right]e_{\text{g}}^{2}\\&\quad+\left[q_{\text{E1}}+\frac{q_{\text{E1}}}{q_{\text{E2}}}\kappa_{\text{g2}}^{2}-\kappa_{\text{g1}}^{2}\text{ch}^{-2}\left(\int_{t_0}^{t}e_{\xi}\left(s\right)\text{d}s\right)\right]e_{\text{g}}\text{th}\left(\int_{t_0}^{t}e_{\xi}\left(s\right)\text{d}s\right)\\&\quad-\left[q_{\text{E2}}\kappa_{\text{f1}}+\kappa_{\text{g2}}\kappa_{\text{f3}}-\kappa_{\text{g1}}\kappa_{\text{g2}}\text{ch}^{-2}\left(\int_{t_0}^{t}e_{\xi}\left(s\right)\text{d}s\right)\right]e_{\text{g}}\text{th}\left(e_{\text{f}}\right)\\&\quad-q_{\text{E1}}\kappa_{\text{g1}}\text{th}^{2}\left(\int_{t_0}^{t}e_{\xi}\left(s\right)\text{d}s\right)-q_{\text{E2}}\kappa_{\text{f3}}\text{th}^{2}\left(e_{\text{f}}\right)\end{aligned}\tag{56}$$

Then, for designing control input u, choose the Lyapunov function for entire system (9) as:

$$V_3\left(\boldsymbol{x},\tilde{\theta},e_{\text{f}},e_{\text{g}}\right)=V_2\left(\boldsymbol{x},\tilde{\theta}\right)+V_{\text{ex}}\left(e_{\text{f}},e_{g}\right)\tag{57}$$

Design control input u so that Equations (17) and (19) are satisfied. Then, differentiate V_3 along the trajectory given by (9) and (17):

$$\begin{aligned}\dot{V}_3\left(\boldsymbol{x},\tilde{\theta},e_{\text{f}},e_{\text{g}}\right)&=\dot{V}_2\left(\boldsymbol{x},\tilde{\theta}\right)+\dot{V}_{\text{ex}}\left(e_{\text{f}},e_{g}\right)\\&\le-\frac{\beta\left(x_1-x_2\right)^2}{\left(n_{\text{r0}}+x_1\right)\left(n_{\text{r0}}+x_1\right)}-G_{\text{r}}\varepsilon_{\text{NP}}x_1^2-\left(1-\gamma\right)\left(1-\eta\right)\frac{q_{\text{R}}}{P_0}\left[\Omega_{\text{P}}\left(x_3-x_4\right)^2+\Omega_{\text{S}}x_4^2\right]\\&\quad-\left(1-\gamma\right)\eta\left(\Omega_{\text{P}}+\Omega_{\text{S}}\right)\frac{q_{\text{R}}}{P_0}\left(x_4-\frac{\Omega_{\text{P}}}{\Omega_{\text{P}}+\Omega_{\text{S}}}x_3\right)^2-\frac{q_{\text{R}}}{2\Sigma_{\text{R}}}\left\{x_3^2+\left[x_3-\Sigma_{\text{R}}\left(1+\frac{\alpha_{\text{R}}}{q_{\text{R}}}\right)x_1\right]^2\right\}\\&\quad-\left[\kappa_{\text{g2}}\kappa_{\text{f1}}-\kappa_{\text{g1}}\text{ch}^{-2}\left(\int_{t_0}^{t}e_{\xi}\left(s\right)\text{d}s\right)\right]e_{\text{g}}^2-k_{\text{g}}e_{\text{g}}\text{th}\left(e_{\text{g}}\right)-q_{\text{E1}}\kappa_{\text{g1}}\text{th}^2\left(\int_{t_0}^{t}e_{\xi}\left(s\right)\text{d}s\right)\\&\quad-q_{\text{E2}}\kappa_{\text{f3}}\text{th}^2\left(e_{\text{f}}\right)+G_{\text{r}}x_1e_{\text{g}}-G_{\text{r}}\kappa_{\text{g1}}x_1\text{th}\left(\int_{t_0}^{t}e_{\xi}\left(s\right)\text{d}s\right)-G_{\text{r}}\kappa_{\text{g2}}x_1\text{th}\left(e_{\text{f}}\right)+e_{\text{g}}w\\&\le-\frac{\beta\left(x_1-x_2\right)^2}{\left(n_{\text{r0}}+x_1\right)\left(n_{\text{r0}}+x_1\right)}-\frac{G_{\text{r}}\varepsilon_{\text{NP}}}{4}x_1^2-\left(1-\gamma\right)\left(1-\eta\right)\frac{q_{\text{R}}}{P_0}\left[\Omega_{\text{P}}\left(x_3-x_4\right)^2+\Omega_{\text{S}}x_4^2\right]\\&\quad-\left(1-\gamma\right)\eta\left(\Omega_{\text{P}}+\Omega_{\text{S}}\right)\frac{q_{\text{R}}}{P_0}\left(x_4-\frac{\Omega_{\text{P}}}{\Omega_{\text{P}}+\Omega_{\text{S}}}x_3\right)^2-\frac{q_{\text{R}}}{2\Sigma_{\text{R}}}\left\{x_3^2+\left[x_3-\Sigma_{\text{R}}\left(1+\frac{\alpha_{\text{R}}}{q_{\text{R}}}\right)x_1\right]^2\right\}\\&\quad-\left[\kappa_{\text{g2}}\kappa_{\text{f1}}-\kappa_{\text{g1}}\text{ch}^{-2}\left(\int_{t_0}^{t}e_{\xi}\left(s\right)\text{d}s\right)-\frac{G_{\text{r}}}{\varepsilon_{\text{NP}}}-\frac{\gamma_{\text{w}}}{4}\right]e_{\text{g}}^2-k_{\text{g}}e_{\text{g}}\text{th}\left(e_{\text{g}}\right)\\&\quad-\left(q_{\text{E1}}\kappa_{\text{g1}}-\frac{G_{\text{r}}}{\varepsilon_{\text{NP}}}\kappa_{\text{g1}}^2\right)\text{th}^2\left(\int_{t_0}^{t}e_{\xi}\left(s\right)\text{d}s\right)-\left(q_{\text{E2}}\kappa_{\text{f3}}-\frac{G_{\text{r}}}{\varepsilon_{\text{NP}}}\kappa_{\text{g2}}^2\right)\text{th}^2\left(e_{\text{f}}\right)+\frac{w^2}{\gamma_{\text{w}}}\end{aligned}\tag{58}$$

where:

$$w=\text{sat}\left(\dot{\xi}_{\text{d}}\right)-\dot{\xi}_{\text{d}}\tag{59}$$

and function sat(·) is determined by (23).

From inequality (58), and by regarding w as the disturbance, it is clear that the closed-loop system is input-to-state stable if inequalities (31), (32) and (33) are all satisfied, which completes the proof of this theorem.

Remark 4. From inequality (58), it is very clear that positive constant γ_w is larger, the influence of *w* is weaker, which then leads to stronger robustness of closed-loop stability to disturbance *w*.

Remark 5. If $w = 0$, *i.e.*:

$$u_{\min} - u_{\mathrm{cp}} \le \dot{\xi}_{\mathrm{d}} \le u_{\max} - u_{\mathrm{cp}} \tag{60}$$

then from inequality (58), we have:

$$\begin{aligned}\dot{V}_3\left(\boldsymbol{x},\tilde{\theta},e_{\mathrm{f}},e_{\mathrm{g}}\right) \le & -\frac{\beta\left(x_1-x_2\right)^2}{\left(n_{\mathrm{r0}}+x_1\right)\left(n_{\mathrm{r0}}+x_1\right)} - \frac{G_{\mathrm{r}}\varepsilon_{\mathrm{NP}}}{4}x_1^2 - (1-\gamma)(1-\eta)\frac{q_{\mathrm{R}}}{P_0}\left[\Omega_{\mathrm{P}}\left(x_3-x_4\right)^2+\Omega_{\mathrm{S}}x_4^2\right] \\ & -(1-\gamma)\eta\left(\Omega_{\mathrm{P}}+\Omega_{\mathrm{S}}\right)\frac{q_{\mathrm{R}}}{P_0}\left(x_4-\frac{\Omega_{\mathrm{P}}}{\Omega_{\mathrm{P}}+\Omega_{\mathrm{S}}}x_3\right)^2 - \frac{q_{\mathrm{R}}}{2\Sigma_{\mathrm{R}}}\left\{x_3^2+\left[x_3-\Sigma_{\mathrm{R}}\left(1+\frac{\alpha_{\mathrm{R}}}{q_{\mathrm{R}}}\right)x_1\right]^2\right\} \\ & -\left[\kappa_{\mathrm{g2}}\kappa_{\mathrm{f1}}-\kappa_{\mathrm{g1}}\mathrm{ch}^{-2}\left(\int_{t_0}^{t}e_{\xi}(s)\,\mathrm{d}s\right)-\frac{G_{\mathrm{r}}}{\varepsilon_{\mathrm{NP}}}\right]e_{\mathrm{g}}^2 - k_{\mathrm{g}}e_{\mathrm{g}}\mathrm{th}\left(e_{\mathrm{g}}\right) \\ & -\left(q_{\mathrm{E1}}\kappa_{\mathrm{g1}}-\frac{G_{\mathrm{r}}}{\varepsilon_{\mathrm{NP}}}\kappa_{\mathrm{g1}}^2\right)\mathrm{th}^2\left(\int_{t_0}^{t}e_{\xi}(s)\,\mathrm{d}s\right) - \left(q_{\mathrm{E2}}\kappa_{\mathrm{f3}}-\frac{G_{\mathrm{r}}}{\varepsilon_{\mathrm{NP}}}\kappa_{\mathrm{g2}}^2\right)\mathrm{th}^2\left(e_{\mathrm{f}}\right)\end{aligned} \tag{61}$$

which means that $\boldsymbol{x}\to\boldsymbol{O}$, $e_{\mathrm{g}}\to 0$, $e_{\mathrm{f}}\to 0$ and $e_{\xi}\to 0$ as $t\to\infty$.

4. Simulation Results with Discussion

In order to show the feasibility of the saturated adaptive output-feedback control law proposed in the above sections, it is applied to the power-level regulation for the MHTGR of the HTR-PM plant in this section. Numerical simulation results corresponding to different cases and control parameters are shown, and some discussions are also given.

4.1. Description of the Numerical Simulation

The dynamic model of the MHTGR utilized in this simulation adopts that one composed of both nodal neutron kinetics and nodal reactor thermal-hydraulics given in [20]. The OTSG model is just the moving boundary model presented in [21]. Furthermore, the model of the steam turbine and that of the electrical generator are also included in the simulation code [22]. The structure of the closed-loop given by this model and the saturated adaptive output-feedback power-level control proposed in this paper is shown in Figure 3. In this simulation, we choose the controller parameters as $k_{\mathrm{NP}} = 2.0$, $k_{\mathrm{NI}} = 2.0$, $q_{\mathrm{R}} = 0.1G_{\mathrm{r}}$, $\gamma = \eta = 0.5$, $\pi_1 = 0.001$, $\pi_2 = 0.01$, $\kappa_{\mathrm{g}i} = 0.001$ ($i = 1, 2$), $\kappa_{\mathrm{f1}} = 0.001$, $\kappa_{\mathrm{f3}} = 0.1$, $q_{\mathrm{E1}} = 0.001$ and $q_{\mathrm{E2}} = 3.0$. Moreover,

$$u_{\max} = -u_{\min} = u_{\mathrm{m}} \tag{62}$$

is adopted here, and u_{m} is set to be different values to see its influence to the control performance.

Figure 3. Schematic view of the closed-loop structure.

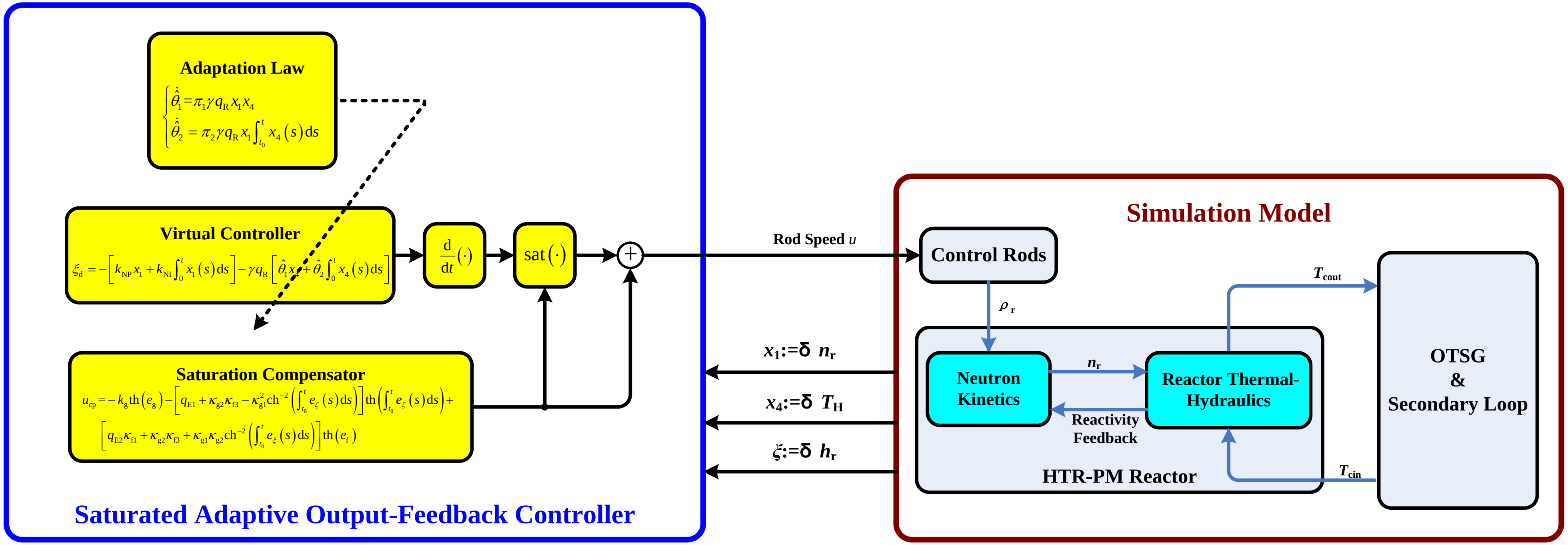

4.2. Simulation Results

The following two case studies are performed here to show the feasibility of the newly-built control.

4.2.1. Case A: Large-Scale Power-Demand Increase

The power-demand signal of an MHTGR of the HTR-PM plant changes linearly from 50% reactor full power (RFP) to 100% RFP with a constant speed of 10%RFP/min, which represents a hard operation of the MHTGR. The dynamic responses of the relative nuclear power n_r, average temperature of the fuel elements T_f, outlet helium temperature T_{cout}, and error signal e_ξ between ξ and ξ_d are given in Figure 4, and moreover the designed control rod speed signal u and compensating signal u_{cp} are also shown in this figure.

Figure 4. Simulation results in case A: (**a**) relative nuclear power n_r; (**b**) average fuel temperature T_f; (**c**) outlet helium temperature T_{cout}; (**d**) error signal e_ξ between ξ and ξ_d; (**e**) designed control rod speed signal u and (**f**) compensating signal u_{cp}.

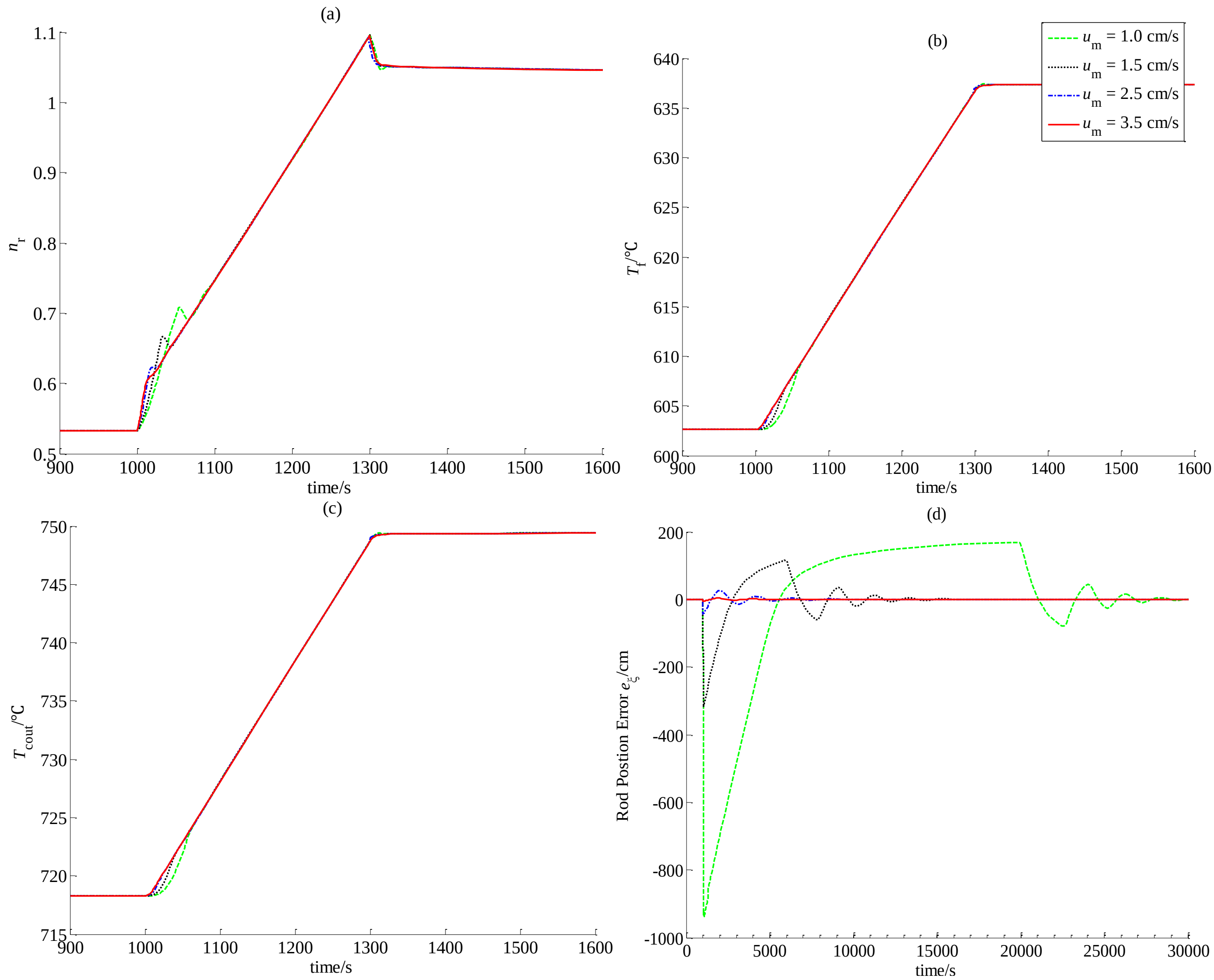

Figure 4. *Cont.*

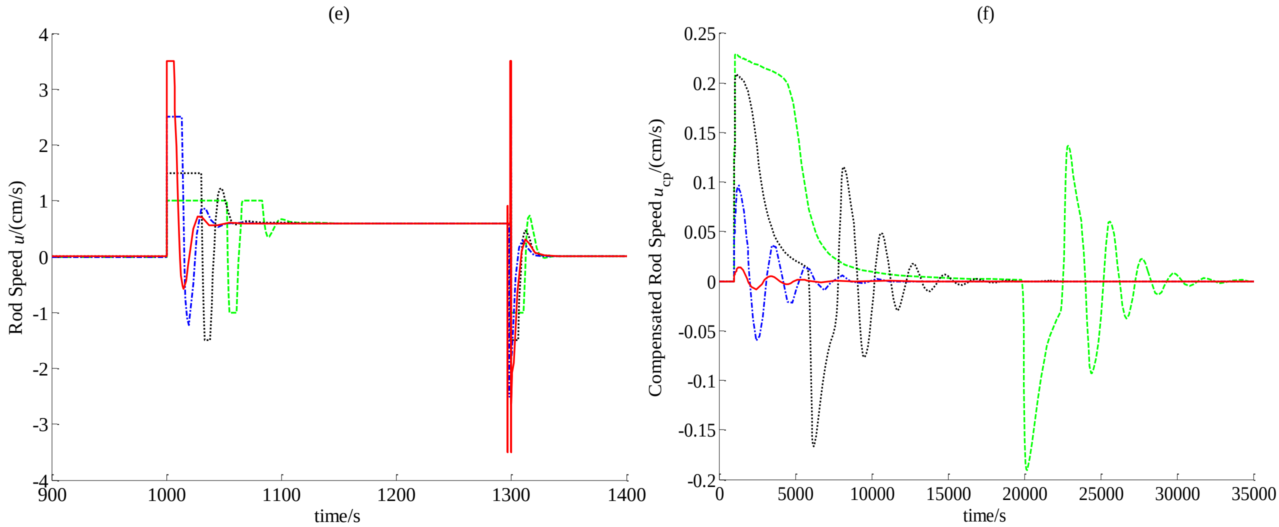

4.2.2. Case B: Large-Scale Power-Demand Decrease

The power-demand signal of the MHTGR decreases linearly from 100% to 50% RFP with a constant speed of 10%RFP/min, which also gives a hard operation of the MHTGR. The dynamic responses of the relative nuclear power, average fuel temperature, outlet helium temperature, and error signal e_ξ and both u and u_{cp} are illustrated in Figure 5.

Figure 5. Simulation results in case B: (**a**) relative nuclear power n_r; (**b**) average fuel temperature T_f; (**c**) outlet helium temperature T_{cout}; (**d**) error signal e_ξ between ξ and ξ_d; (**e**) designed control rod speed signal u and (**f**) compensating signal u_{cp}.

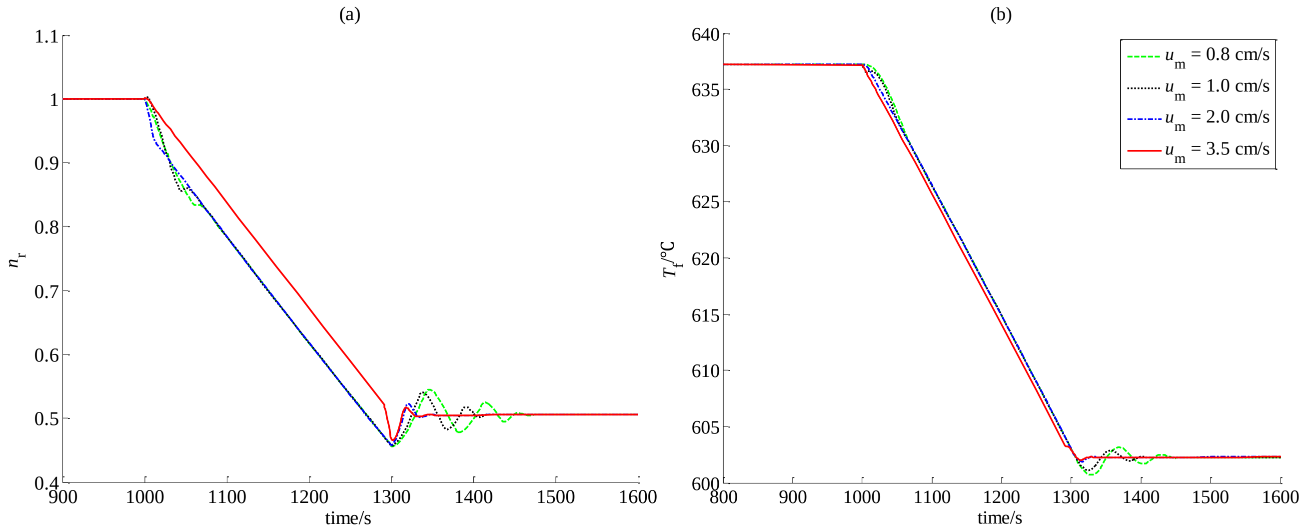

Figure 5. *Cont.*

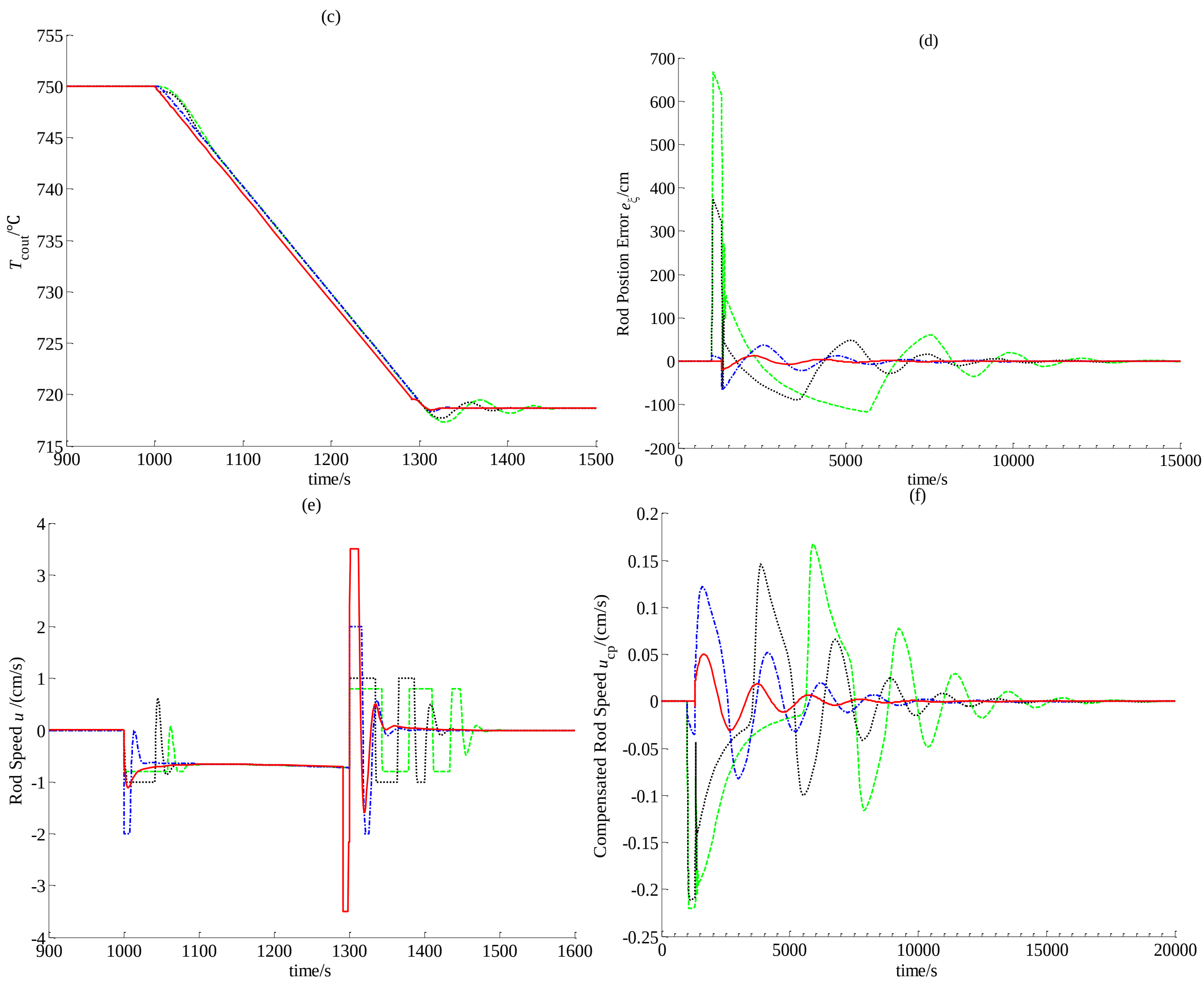

4.3. Discussion

The power-demand determines the setpoints of the relative nuclear power and average temperature of the helium flow inside the primary loop. Suppose that the MHTGR operates at a steady state for a certain period before the power-demand changes. It is clear that the variation of the power-demand signal enlarge the errors between actual values and setpoints of the nuclear power and helium temperature, *i.e.*, measurable state-variables x_1 and x_4 defined by Equation (5). Further, from Equation (18), the variations of x_1 and x_4 determine the variation of ξ_d, which in turn enlarge e_ξ defined by (22). Then, x_1, x_4 and e_ξ derives the newly-built saturated adaptive control law given by Equations (17), (19)–(21), (26) and (27) to generate saturated control rod speed signal so that the MHTGR can come to the newly given power-level.

From the simulation results illustrated by Figures 4 and 5, we can see that the closed-loop stability is well guaranteed, which provides a satisfactory dynamic performance for the MHTGR. Moreover, from parts (a), (b) and (c) of Figures 4 and 5, the control performance is better if the saturation bound u_m is larger. The reason is that as u_m becomes larger, the control rods can move faster, which means that the control errors and disturbances can be suppressed faster and more efficiently. Actually, through corresponding parts (a), (b) and (c) to part (d) of Figures 4 and 5, it is clear that there is a trade-off between the response quality level and saturation bound u_m. Furthermore, from part (d) of Figures 4 and 5, saturation bound u_m is smaller, the mismatch between ξ and ξ_d, *i.e.*, e_ξ is larger, and however the closed-loop stability is still guaranteed, which is given by compensation effect caused by term u_{cp} determined by Equations (19)–(21). As we can see from part (f) of Figures 4 and 5, the compensating effect generated by u_{cp} is stronger if u_m is smaller, and is dissipated as the entire system converges to a given steady state.

Finally, from the theoretical analysis in the above section and the numerical simulation in this section, the newly-built saturated adaptive power-level controller of the MHTGR guarantees satisfactory closed-loop stability and reactor operability. Thanks to the widely utilization of advanced digital control system platforms, there is no difficulty in realizing this novel control law. In the practical engineering, the startup of a SMR is usually performed by the operators. After the startup, an automatic reactor control system can be permitted to switch on. Therefore, the power-level controller given in this paper is designed for normal power operation, and NOT for reactor startup.

5. Conclusions

MHTGR has already been seen as one of the best candidates for building SMR-based nuclear power plants with both inherent safety features and potential economic competitive power. Power-level control is very crucial in providing safe, stable and efficient operation for MHTGRs. However, since there exists nonlinearity, parameter uncertainty and input saturation in MHTGR-based nuclear plant dynamics, it is necessary to provide a nonlinear adaptive power-level control design method with saturation compensating function. In this paper, a novel saturated adaptive output-feedback power-level control for MHTGRs is proposed. It is proved theoretically that this control law can provide input-to-state stability (ISS) for the closed-loop system. The novelties in developing the control include: (1) constructing Lyapunov function based upon the shifted-ectropies of both reactor neutron kinetics and thermal-hydraulics so that this control has a neat form; (2) giving an adaptation law for this control so that its parameters can be tuned online; and (3) proposing a saturation compensating algorithm so that the closed-loop ISS can be realized by saturated control input. Furthermore, numerical simulation results in the cases of large-range power-level increase and decrease not only verify the theoretic results but also illustrate the relationship between regulating performance and control input bound. Finally, this newly-built power-level controller can be easily implemented on advanced digital control system platforms for possible engineering applications. It is well known that different fuel types induce different values of the fraction of the delayed neutrons β [23,24], which in turn influence the reactor dynamics deeply. In the future, the impact of different β to power-level control design should be studied, and the corresponding adaptive power-level control law should be designed.

Acknowledgments

The work in this paper is jointly supported by Natural Science Foundation of China (NSFC) (Grant No. 61374045), Tsinghua University Initiative Scientific Research Program (Grant No. 20121087992) and National S&T Major Project (Grant No. ZX06901). Moreover, the author would like to thank Huang Xiao-Jin deeply for consistent support, valuable discussions and constructive suggestions.

Conflicts of Interest

The author declare no conflict of interest.

References

1. Ingersoll, D.T. Deliberately small reactors and the second nuclear era. *Prog. Nuclear Energy* **2009**, *51*, 589–603.
2. Vujić, J.; Bergmann, R.M.; Škoda, R.; Miletić, M. Small modular reactors: simpler, safer, cheaper? *Energy* **2012**, *45*, 288–295.
3. Lohnert, G.H. Technical design features and essential safety-related properties of the HTR-Module. *Nuclear Eng. Des.* **1990**, *121*, 259–275.
4. Wu, Z.; Lin, D.; Zhong, D. The design features of the HTR-10. *Nuclear Eng. Des.* **2002**, *218*, 25–32.
5. Zhang, Z.; Sun, Y. Economic potential of modular reactor nuclear power plants based on the Chinese HTR-PM project. *Nuclear Eng. Des.* **2007**, *237*, 2265–2274.
6. Zhang, Z.; Wu, Z.; Wang, D.; Xu, Y.; Sun, Y.; Li, F.; Dong, Y. Current status and technical description of Chinese 2 × 250 MW_{th} HTR-PM demonstration plant. *Nuclear Eng. Des.* **2009**, *239*, 265–2274.
7. Li, W.; Zhang, Y.; Zheng, W. Investigation on three seawater desalination process coupled with NHR-200. *Desalination* **2012**, *298*, 93–98.
8. Zhang, P.; Chen, S.Z.; Wang, L.J.; Xu, J.M. Overview of nuclear hydrogen production research through iodine sulfur process at INET. *Int. J. Hydrog. Energy* **2010**, *35*, 2883–2887.
9. Shtessel, Y.B. Sliding mode control of the space nuclear reactor system. *IEEE Trans. Aerosp. Electron. Syst.* **1998**, *34*, 579–589.
10. Etchepareborda, A.; Lolich, J. Research reactor power controller design using an output feedback nonlinear receding horizon control method. *Nuclear Eng. Des.* **2007**, *237*, 268–276.
11. Eliasi, H.; Menhaj, M.B.; Davilu, H. Robust nonlinear model predictive control for nuclear power plants in load following operations with bounded xenon oscillations. *Nuclear Eng. Des.* **2011**, *241*, 533–543.
12. Eliasi, H.; Menhaj, M.B.; Davilu, H. Robust nonlinear model predictive control for a PWR nuclear power plant. *Prog. Nuclear Energy* **2012**, *54*, 177–185.
13. Dong, Z. Dynamic output feedback power-level control for the MHTGR based on iterative damping assignment. *Energies* **2012**, *5*, 1782–1815.
14. Kokotović, P. The joy of feedback. *IEEE Control Syst.* **1992**, *12*, 7–17.
15. Dong, Z. Physically-based power-level control for modular high temperature gas-cooled reactors. *IEEE Trans. Nuclear Sci.* **2012**, *59*, 2531–2549.
16. Park, M.G.; Cho, N.Z. Time-optimal control of nuclear reactor power with adaptive proportional-integral-feedforward gains. *IEEE Trans. Nuclear Sci.* **1993**, *40*, 266–270.
17. Arab-Alibeik, H.; Setayeshi, S. Adaptive control of a PWR core power using neural networks. *Ann. Nuclear Energy* **2005**, *32*, 588–605.

18. Dong, Z. Artificial neural network compensated output feedback power-level control for modular high temperature gas-cooled reactors. *Energies* **2014**, *7*, 1149–1170.
19. Sontag, E.D. Input to state stability: basic concepts and results. In *Nonlinear and Optimal Control Theory*; Cachan, J.M., Groningen, F.T., Paris, B.T., Eds.; Springer: Berlin, Germany, 2008; pp. 163–220.
20. Dong, Z.; Huang, X.; Zhang, L. A nodal dynamic model for control system design and simulation of an MHTGR core. *Nuclear Eng. Des.* **2010**, *240*, 1251–1261.
21. Li, H.; Huang, X.; Zhang, L. A lumped parameter dynamic model of the helical coiled once-through steam generator with movable boundaries. *Nuclear Eng. Des.* **2008**, *238*, 1657–1663.
22. Dong, Z.; Huang, X. Real-Time Simulation Platform for the Design and Verification of the Operation Strategy of the HTR-PM. In Proceedings of the 21th International Conference on Nuclear Engineering, Chengdu, China, 29 July–2 August 2013; ICONE21–16023.
23. Mazzini, G.; Bomboni, E.; Cerullo, N.; Fridman, E.; Lomonaco, G.; Shwageraus, E. The use of Th in HTR: state of the art and implementation in Th/Pu fuel cycles. *Sci. Technol. Nuclear Install.* **2009**, doi:10.1155/2009/749736.
24. Cerullo, N.; Bufalino, D.; Forasassi, G.; Lomonaco, G.; Rocchi, P.; Romanello, V. An additional performance of HTRs: The waste radiotoxicity minimisation. *Radiat. Prot. Dosim.* **2005**, *115*, 122–125.